Symposium on Recent Advances in Structural Engineering, Mechanics and Materials
In Honor of Professor Pisidhi Karasudhi, August 4-5, 2006

ELASTODYNAMIC RECIPROCITY RELATIONS FOR WAVE SCATTERING PROBLEMS IN COMPOSITE PLATES

W. KARUNASENA[1]

ABSTRACT: Due to the low density, high performance and increased service life, composite materials are receiving wider attention in civil, mechanical and aerospace engineering applications. In this paper, we develop elastodynamic reciprocity relations for wave scattering by flaws (such as cracks and delaminations) when guided waves are allowed to propagate in fibre-reinforced composite plates. These relations are useful to check the accuracy of the numerical solution for the scattered wave field. It is well known that scattered wave field provides very useful information for ultrasonic non-destructive assessment of flaws in composite structures. The classical elastodynamic reciprocity theorem is used to derive simple reciprocity relations for reflected and transmitted wave amplitudes and the corresponding energies associated with the wave modes. A hybrid method is used for solving the wave scattering problem. The hybrid method combines a finite element formulation in the interior region that consists of the flaw and a finite region of the plate around the flaw with a wave function expansion representation in the unbounded exterior regions. The analysis is presented for a plate with an arbitrary stacking sequence where each ply can have an arbitrary fibre direction. The derived reciprocity relations are used to check the accuracy of the numerical solution for several example scattering problems.

KEYWORDS: reciprocity relations, wave scattering, composite plates, hybrid method, guided waves, cracks, delaminations, finite elements, reflection and transmission coefficients.

1. INTRODUCTION

In the last two decades, fiber-reinforced composite materials, specially fiber-reinforced plastics (abbreviated as FRPs), have been receiving wide attention in aerospace, civil and mechanical engineering applications due to their useful properties such as light weight, high strength, corrosion resistance and long term durability. A state-of-the-art-review of FRP composites for construction applications can be found in [1]. It is well known that structural integrity of facilities made from FRPs are severely affected by flaws such as cracks and delaminations developed within the FRP part of the structure. Guided elastic waves in plate-like composite parts possess characteristics that make them particularly useful for applications in non-destructive evaluation of flaws in composite structures. When excited at a particular location in a plate, guided waves can travel long distances along the plate and when they meet a flaw along their path, the waves start scattering. The scattered wave, which can travel long distances along the plate, will carry information about the size and location of the flaw, thus providing an ultrasonic non-destructive means of inspection of an otherwise inaccessible area of

[1] *Senior Lecturer, James Cook University, Australia*

the structure. Ultrasonic non-destructive evaluation methods heavily rely on the solution to the wave scattering problem that happens at the flaw.

Obtaining closed-form solutions to even the simplest wave scattering problems in composite plates is not practical if not impossible. A numerical method for obtaining a solution to the scattered wave field is quite intricate and complicated, and as a result, the accuracy of a numerically obtained solution is questionable. One way of overcoming this problem is having some indicators based on sound theories to check the accuracy of the numerical solution. The satisfaction of elastodynamic reciprocity relations serves as one such indicator of the accuracy of the solution for the wave scattering problem.

Chimenti [2] has published a comprehensive review of guided waves in composite plates and their use for non-destructive material characteristion. Recently, Datta [3] provided a detailed review of the theory of guided waves in composite plates and shells. Although a vast body of work on guided ultrasonic wave propagation in plates and shells now exists, relatively few studies have dealt with scattering of these waves by cracks and delaminations. Moreover, these few studies have been mostly confined to the problems of horizontally polarized shear (SH) waves and plane strain (two-dimensional) waves. The author and his co-workers [4] have investigated the two-dimensional wave scattering by a symmetric normal surface breaking crack in a cross-ply laminated plate by using a hybrid method which combines finite element method with wave function expansion procedure.

Recently, author [5] extended the hybrid method to provide a model analysis of scattering of a guided wave incident obliquely on a long symmetric surface breaking crack in a composite plate. The solution to this problem is the first step towards analyzing the general three-dimensional scattering in a composite plate. In this paper, we present the derivation of elastodynamic reciprocity relations for the scattering problem of a guided wave incident obliquely on a long flaw in a composite plate. The analysis is presented for a plate with an arbitrary stacking sequence where each ply can have arbitrary fiber direction with respect to the global coordinate system. Numerical results for reciprocity relations are provided for three special cases – (i) scattering by a symmetric normal edge crack in a uni-axially fiber-reinforced homogeneous graphite-epoxy composite plate, (ii) scattering by a symmetric normal edge crack in an 8 layer graphite-epoxy cross-ply laminated plate, and (iii) scattering by a thin planar crack located at the fixed-end of a semi-infinite homogeneous composite plate.

2. FORMULATION

2.1 SCATTERING PROBLEM

Time harmonic wave scattering of a guided plate wave incident obliquely on a flaw in a composite plate as shown in Figure 1 is considered. The composite material in the plate is uni-axially fibre-reinforced within each layer (or ply or lamina) and possibly laminated with each ply having an arbitrary fibre-direction with respect to the global x-direction. Each layer lies on a plane parallel to x-y plane. It is assumed that all layers of the plate have equal thickness with transversely isotropic elastic properties. The flaw is located at $x = 0$ and is assumed to be very long (in comparison to the plate thickness) in y-direction. It has a constant cross-section in x-z plane. It is assumed that two faces of the plate $z = 0$ and $z = H$ are stress free. Also, the flaw surface is assumed to be open with zero traction. Since the direction of the flaw (i.e. y-direction in this case), in general, is not known *a priori,* it is not always possible to excite the incident wave in the x-direction. Therefore, it is necessary to consider the general case where the incident wave is propagating at an arbitrary angle to x-direction and fibre direction is also at an arbitrary angle to global x-direction. Let the incident wave be a guided plate wave mode travelling at a direction making an angle $90^0 - \phi^{in}$ with the y-z plane and fibres are at an angle θ to the x-direction.

When the incident wave mode strikes the flaw, mode conversion will happen and a scattered field consisting of reflected and transmitted plate wave modes will be generated. The aim of this work is to numerically quantify this scattered field and derive reciprocity relations applicable to converted modes for the purpose of checking the accuracy of the numerical solution for the scattered wave field. In general, the incident and the scattered wave field will have all three displacement components in the x, y, and z directions. Let u(x,y,z,t), v(x,y,z,t), and w(x,y,z,t) denote the displacement quantities in x, y, and z directions, respectively. Here t denotes time.

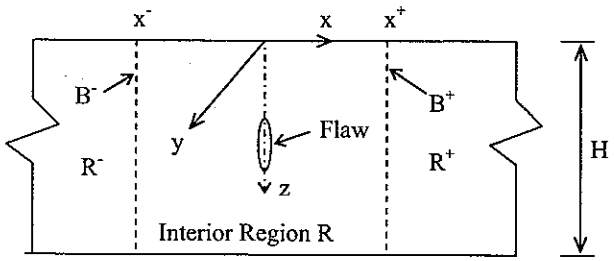

Figure 1. Geometry of the Problem

2.2 SOLUTION FOR SCATTERING PROBLEM

The hybrid method described in [4, 5] is adopted for solving this scattering problem. The hybrid combines finite element formulation in a bounded interior region of the plate with a wave function expansion representation in the exterior region. The regions are connected along vertical boundaries B^+ at $x = x^+$, and B^- at $x = x^-$ as shown in Figure 1. Let κ be the wave number of the incident wave in the direction of propagation. Thus, κ should be one of the admissible real roots of the dispersion equation for off-axis propagation. Since the flaw extends to infinity in y-direction, the scattered field must have the same wave number in the y-direction as the incident field. Thus, each of the scattered wave modes will have a constant wave number η_0 ($= \kappa \text{ Sin } \phi^{in}$) in the negative y direction. Therefore, for time-harmonic waves, y and t variation can be factored out as

$$\begin{Bmatrix} u(x,y,z,t) \\ v(x,y,z,t) \\ w(x,y,z,t) \end{Bmatrix} = \begin{Bmatrix} \hat{u}(x,z) \\ \hat{v}(x,z) \\ \hat{w}(x,z) \end{Bmatrix} \exp[-j(\eta_0 y + \omega t)] \tag{1}$$

where ω is the circular frequency and $j = \sqrt{-1}$.

The procedure for finite element formulation for the interior region R for is very similar to that for the plane strain case given in [4]. The finite element representation of the interior region should include singular elements at crack tips if the flaw considered is a crack or a delamination. The standard discretization process in the finite element method leads to

$$\delta\{\overline{q}\}^T[S]\{q\} - \delta\{\overline{q}_B\}^T\{P_B\} = 0 \tag{2}$$

where

$$[S] = [K] - \omega^2[M] \tag{3}$$

in which: [K] and [M] are, respectively, the global stiffness and mass matrices of the interior region; {q} is the nodal displacement vector corresponding to interior nodes; and $\{q_B\}$ and $\{P_B\}$ are, respectively, the nodal displacement vector and the interaction force vector corresponding to the boundary nodes. δ implies first variation and overbar denotes complex conjugate.

The wave field in the exterior regions R^+ and R^- is the superposition of those due to the incident wave and the scattered waves. Using the wave function expansion, the scattered wave field can be expressed in terms of the wave functions (ie wave modes) supported by the free infinite composite plate with no flaws and the unknown reflected and transmitted wave amplitudes. The theoretical details of the methodology adopted to obtain wave functions can be found in our work reported in [6]. The procedure starts with dividing each layer into several sub-layers. The exact dispersion relation of the infinite plate is developed using the propagator matrices as

$$f(\omega, k) = 0 \tag{4}$$

where k denotes the x-direction wave number of a typical wave mode. It is well known that the plate wave modes are dispersive and at any given frequency ω, there are only a finite number of propagating modes that carry energy away from a source of excitation or upon scattering from an inhomogeneity or flaw. However, in order to satisfy the boundary conditions at the source or at a boundary of discontinuity it is necessary to include also the non-propagating modes in the modal representation of the displacement field. The wave numbers (k) for the propagating and non-propagating modes at a given frequency of excitation can be found by solving the dispersion equation (4) for the plate. For each wave number k, the corresponding displacement wave function (which is basically a vector containing x and z direction displacement at each sub-layer level) can be determined using the propagator matrix for each sub-layer. This has been discussed in the references cited above.

The solution to the scattering problem is obtained by imposing the continuity of total (incident plus scattered) displacements and tractions on the boundaries. This is achieved by substituting for $\{q_B\}$ and $\{P_B\}$ from the wave function expansion into equation (2). This leads to a system of linear equations to solve for the unknown reflected wave amplitudes (A_m^+) and transmitted amplitudes (A_m^-). These amplitudes are then used to obtain boundary nodal displacements and, in turn, to obtain interior nodal displacements. The reflection coefficient R_{pm} of the m-th reflected mode and transmission coefficient T_{pm} of the m-th transmitted mode, due to the p-th incident wave mode, are given by

$$R_{pm} = A_m^+ / A_p^{in}, \qquad T_{pm} = \begin{cases} A_m^- / A_p^{in} & \text{for } m \neq p \\ (A_p^{in} + A_m^-) / A_p^{in} & \text{for } m = p \end{cases} \tag{5}$$

in which, A_p^{in} is the amplitude of the incident wave mode.

2.3 RECIPROCITY RELATIONS

The reciprocity relations are derived from the elastodynamic reciprocity theorem [7-8], which may be written using the usual tensor notation, in the absence of body forces, as

$$\oint_S (u_j^B \sigma_{jk}^A - u_j^A \sigma_{jk}^B) n_k \, dS = 0, \qquad j,k = x,y,z \tag{6}$$

where u_j^A and σ_{jk}^A represent the displacements and stresses corresponding to elastodynamic state A while u_j^B and σ_{jk}^B are the displacements and stresses corresponding to elastodynamic state B, in a

region V bounded by a surface S. Wave fields corresponding to both elastodynamic states vary harmonically in time with circular frequency ω. When writing equation (6), Einstein's summation convention of repeated indices has been assumed to hold, and the displacement components u, v, w have been represented by u_x, u_y, u_z respectively. In order to derive reciprocity relations, the orthogonality relations among the wave modes have to be established first.

For convenience in derivation of orthogonality relations, few notations are introduced first. Let the wave number pair (k_n,ζ_0) denote a admissible wave mode propagating in the first quadrant of x-y plane in an infinite composite plate with no flaws. Herein, k_n represents the positive x direction wave number and ζ_0 (which is fixed) represents the positive y direction wave number as opposed to the definition in of η_0 in equation (1). Note that $\eta_0 = -\zeta_0$. In a similar manner, let the wave number pairs $(-k_n^*,\zeta_0)$, $(-k_n,-\zeta_0)$, and $(k_n^*,-\zeta_0)$ denote the wave modes corresponding to second, third and fourth quadrants of the x-y plane, respectively. It should be mentioned here that if (k_n,ζ_0)-th wave mode is an admissible wave mode (of the dispersion relation of the plate), then $(-k_n,-\zeta_0)$-th wave mode, which is propagating in the opposite direction, is also an admissible wave mode. Similarly, if $(k_n^*,-\zeta_0)$-th wave mode is admissible, then $(-k_n^*,\zeta_0)$-th wave mode is also admissible. This point can be explained by visualising the configuration of the plate with respect to a new coordinate system that is obtained after rotating the x,y axes by 180^0 about the z axis. However, when (k_n,ζ_0)-th wave mode is an admissible wave mode, $(k_n,-\zeta_0)$-th wave mode is not necessarily an admissible wave mode. Due to this reason, a superscript star $(^*)$ has been introduced to the x-direction wave numbers of wave modes corresponding to second and fourth quadrants of the x-y plane. Note that $(k_n,-\zeta_0)$-th wave mode is admissible when the fibres in each layer are aligned either in x or y directions. This can be visualised by considering the mirror image of the plate with respect to the x-z plane.

The orthogonality relations are derived by applying the reciprocity theorem to the close region V bounded by planes z = 0, z = H, $x = x_1$, $x = x_2$, $y = y_1$, and $y = y_2$ where x_1, x_2, y_1 and y_2 are coordinates chosen in such a way that $x_2 > x_1$ and $y_2 > y_1$. State A is taken to be the field due to $(-k_n^*,\zeta_0)$-th wave mode and state B is taken to be the field due to $(k_m^*,-\zeta_0)$-th wave mode. Then, the wave fields due to two states can be written as

$$u_j^A \rightarrow A_{-n}^{*+}\{u_{-n}^{*+}\}\exp[j(-k_n^* x + \zeta_0 y)] \tag{7a}$$

$$\sigma_{jk}^A \rightarrow A_{-n}^{*+}\begin{Bmatrix}\{\sigma_{-nx}^{*+}\}\\ \{\sigma_{-ny}^{*+}\}\end{Bmatrix}\exp[j(-k_n^* x + \zeta_0 y)] \tag{7b}$$

$$u_j^B \rightarrow A_m^{*-}\{u_m^{*-}\}\exp[j(k_m^* x - \zeta_0 y)] \tag{7c}$$

$$\sigma_{jk}^B \rightarrow A_m^{*-}\begin{Bmatrix}\{\sigma_{mx}^{*-}\}\\ \{\sigma_{my}^{*-}\}\end{Bmatrix}\exp[j(k_m^* x - \zeta_0 y)] \tag{7d}$$

where A_{-n}^{*+}, $\{u_{-n}^{*+}\}$, $\{\sigma_{-nx}^{*+}\}$ and $\{\sigma_{-ny}^{*+}\}$ represent the amplitude, displacement mode shape vector, mode shape vector of tractions on x face and the mode shape vector of tractions on y face, respectively, for the $(-k_n^*,\zeta_0)$-th wave mode; and A_m^{*-}, $\{u_m^{*-}\}$, $\{\sigma_{mx}^{*-}\}$ and $\{\sigma_{my}^{*-}\}$ represent the same quantities for the $(k_m^*,-\zeta_0)$-th wave mode. Application of elastodynamic reciprocity theorem expressed in mathematical form in equation (6) to the region V for states A and B defined in equations (7) results in

$$\{\exp[j(k_m^* - k_n^*)x_2] - \exp[j(k_m^* - k_n^*)x_1]\}\, I_4[(k_m^*, -\zeta_0);(-k_n^*, \zeta_0)] = 0 \tag{3}$$

where the notation $I_4[(k_m^*, -\zeta_0);(-k_n^*, \zeta_0)]$ has been used to represent the integral

$$\int_0^H (\{u_m^{*-}\}^T \{\sigma_{-nx}^{*+}\} - \{u_{-n}^{*+}\}^T \{\sigma_{mx}^{*-}\})dz.$$

Since x_1 and x_2 are arbitrary, equation (8) leads to the orthogonality relation

$$I_4[(k_m^*, -\zeta_0);(-k_n^*, \zeta_0)] = 0 \quad \text{for } k_m^* \neq k_n^*. \tag{9}$$

It should be noted that the net contributions from the surface integrals in equation (6) on planes $y = y_1$ and $y = y_2$ amount to zero.

In a similar manner, choosing states A and B as the fields due to (k_n,ζ_0)-th and $(-k_m,-\zeta_0)$-th wave modes, respectively, it can be shown that

$$I_4[(-k_m, -\zeta_0);(k_n, \zeta_0)] = 0 \quad \text{for } k_m \neq k_n. \tag{10}$$

Adopting a similar approach, the following orthogonality relations can be derived:

$$I_4[(k_m^*, -\zeta_0);(k_n, \zeta_0)] = 0, \tag{11}$$

$$I_4[(-k_m, -\zeta_0);(-k_n^*, \zeta_0)] = 0. \tag{12}$$

In order to derive reciprocity relations, region V is chosen as the region of the plate surrounding the flaw, bounded by the planar surfaces $z = 0$, $z = H$, $x = x_3$ $(x_3 \geq x^+)$, $x = x_4$ $(x_4 \leq x^-)$, $y = y_1$, and $y = y_2$ (where y_1 and y_2 are arbitrary, and $y_2 > y_1$). The reciprocity relations among reflection coefficients can be derived from equation (6) by choosing state A as the total field due to $(-k_n, -\zeta_0)$-th incident wave mode and state B as the total field due to (k_p^*, ζ_0)-th incident wave mode. Let R_{nq} and T_{nq} denote the reflection and transmission coefficients, respectively, due to $(-k_n, -\zeta_0)$-th incident wave mode; and R_{pm}^* and T_{pm}^* denote the same quantise due to $(-k_p^*, \zeta_0)$-th incident wave mode. In view of orthogonality relations given in equations (9) to (12), the reciprocity relations becomes (after some algebraic manipulations)

$$R_{pn}^* \varsigma_n = R_{np} \varsigma_p^* \tag{13}$$

where

$$\varsigma_n = \int_0^H (\{u_n^+\}^T \{\sigma_{-nx}^-\} - \{u_{-n}^-\}^T \{\sigma_{nx}^+\})dz, \tag{14a}$$

$$\varsigma_p^* = \int_0^H (\{u_p^{*-}\}^T \{\sigma_{-px}^{*-}\} - \{u_{-p}^{*+}\}^T \{\sigma_{px}^{*-}\})dz. \tag{14b}$$

In equation (14), $\{u_n^+\}$, $\{u_{-n}^-\}$, $\{u_p^{*-}\}$ and $\{u_{-p}^{*+}\}$ denote the displacement mode shape vectors corresponding to (k_n,ζ_0)-th, $(-k_n,-\zeta_0)$-th, $(k_p^*,-\zeta_0)$-th and $(-k_p^*,\zeta_0)$-th wave modes, respectively, in an infinite plate with no flaw. The corresponding traction mode shape vectors on the x face denoted by $\{\sigma_{nx}^+\}$, $\{\sigma_{-nx}^-\}$, $\{\sigma_{px}^{*-}\}$ and $\{\sigma_{-px}^{*-}\}$. It should be noted that the net contributions to the surface integral in equation (6) from surfaces $y = y_1$ and $y = y_2$ becomes zero.

Applying the reciprocity theorem to the same region V, with state A as the total field due to (k_n,ζ_0)-th incident mode and state B as the total field due to $(-k_p,-\zeta_0)$-th incident mode, the reciprocity relation among the transmission coefficients can be derived as

$$T_{pn}\varsigma_n = T_{np}\varsigma_p \tag{15}$$

where ς_p is given by equation (14a) with n replaced by p. When deriving equation (15), it has been assumed that the flaw geometry is symmetric with respect to the x = 0 plane. It can be shown that, when the fibres in each layer are either in x or y direction, the reciprocity relation in equation (13) degenerates into

$$R_{pn}\varsigma_n = R_{np}\varsigma_p \tag{16}$$

Let E_{pn}^+ be the proportion of energy of the $(-k_p,-\zeta_0)$-th incident wave mode transferred into the n-th reflected mode during the scattering process. Similarly, let E_{pn}^- be the proportion of incident energy transferred to the n-th transmitted mode. Then, following the procedure adopted for plane strain situation in [4], the final form of the reciprocity relations becomes

$E_{pn}^+ = E_{np}^+$ for the reflected field when fibres are aligned with global x,y directions, (17a)

and

$E_{pn}^- = E_{np}^-$ for the transmitted field for arbitrary fibre directions. (17b)

3. RESULTS AND DISCUSSION

Reciprocity relations derived in the previous section has been used to check the accuracy of three example scattering problems described below:

Example 1: Scattering by a thin symmetric normal edge crack in a uni-axially fibre-reinforced homogeneous graphite-epoxy plate. The geometry of the crack is as shown in Figure 2a.

Example 2: Scattering by a thin symmetric normal edge crack in an 8 layer graphite-epoxy plate with the stacking sequence of $0^0/90^0/0^0/90^0/90^0/0^0/90^0/0^0$. The geometry of the crack is same as that shown in Figure 2a.

Example 3: Scattering by a thin crack located at the fixed-end of a uni-axially fibre-reinforced homogeneous graphite-epoxy plate as shown in Figure 2b.

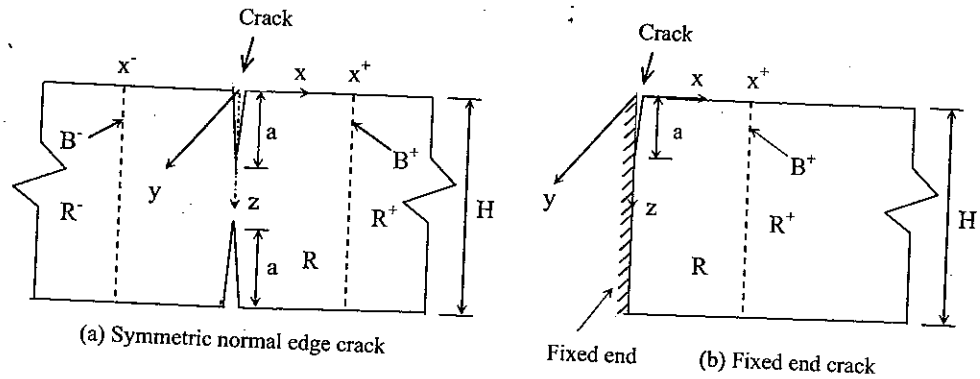

Figure 2. Geometry of the flaws for example problems

The elastic constants (C_{ij}) for the transversely isotropic graphite-epoxy composite material are given in Table 1. More information on C_{ij} constants and their relation to the stiffness matrix in equation (3), and the procedure for their transformation from fibre direction to global x,y directions can be found in [9].

Table 1. Elastic constants of graphite-epoxy lamina (in GPa)

Lamina	C_{11}	C_{33}	C_{13}	C_{55}
0^0	160.73	13.92	6.44	7.07
90^0	13.92	13.92	6.92	3.50

Numerical results from the hybrid method for the magnitudes of reflection and transmission coefficients ($|R_{pn}|$ and $|T_{pn}|$), and proportions of reflected and transmitted energies (E^+_{pn} and E^-_{pn}) for example 1 are presented in Table 2. The results correspond to a normalized frequency Ω $(=\omega H/(2\sqrt{(C_{55}/\rho)_0})$ where ρ is the density of the graphite-epoxy composite) of 2.0 and a normalized crack length (= a/(0.5H)) of 0.1 or 0.5 as given in the table. In this table, p and n denote the incident and the scattered wave mode numbers, respectively, and all incident modes considered are symmetric modes. Note that, due to the symmetry of the problem with respect to the mid-plane of the plate, the scattered wave field consist of only symmetric or anti-symmetric modes depending on whether the incident mode is a symmetric or anti-symmetric one. It can be seen from this table that final form of the reciprocity relations among the proportions of energy as given in equation (17) are satisfied with negligible errors. Also it is seen that some reflection and transmission coefficients are quite sensitive to the orientation and the depth of the crack, and the incident wave mode number. Although not shown here, our computations showed that coefficients are also sensitive to the incident mode frequency. Satisfaction of reciprocity relations can be taken as an indicator of the accuracy of the scattering results.

Table 3 shows the scattering results for the 8 layer composite plate in example 2 at a normalized frequency of 4 and at a normalized crack length of 0.5. It is clearly seen that reciprocity relations in equation (17) are satisfied with negligible errors.

Table 2. Scattering results for example 1 when Ω=2

(a) $\theta = 0^0$, $\varphi^{in} = 45^0$, $\eta_0 = 1.440$

p	k_p	a/(0.5H)	n	E^+_{pn}	E^-_{pn}	$\|R_{pn}\|$	$\|T_{pn}\|$
1	1.440	0.1	1	0.002	0.993	0.044	0.996
			2	0.001	0.001	0.051	0.048
		0.5	1	0.009	0.821	0.095	0.906
			2	0.127	0.042	0.718	0.409
2	0.324	0.1	1	0.001	0.001	0.012	0.012
			2	0.000	0.999	0.011	0.999
		0.5	1	0.128	0.041	0.178	0.101
			2	0.070	0.760	0.264	0.872

(b) $\theta = 22.5^0$, $\varphi^{in} = 22.5^0$, $\eta_0 = 0.780$

p	k_p	a/(0.5H)	n	E^+_{pn}	E^-_{pn}	$\|R_{pn}\|$	$\|T_{pn}\|$
1	1.882	0.1	1	0.000	0.998	0.009	0.999
			2	0.000	0.000	0.062	0.033
		0.5	1	0.002	0.833	0.105	0.913
			2	0.081	0.082	1.357	0.632
2	0.813	0.1	1	0.000	0.000	0.014	0.007
			2	0.000	1.000	0.009	1.000
		0.5	1	0.000	0.082	0.024	0.129
			2	0.075	0.842	0.590	0.918

Note: p and n denote the incident and scattered wave mode numbers, respectively. Symmetric incident wave modes have been considered.

Table 3. Scattering results for example 2 when Ω=4, a/(0.5H)=0.5, θ for 0^0 lamina = 0^0, $\varphi^{in} = 45^0$, and $\eta_0 = 3.362$

p	k_p	n	E^+_{pn}	E^-_{pn}	$\|R_{pn}\|$	$\|T_{pn}\|$
1	3.362	1	0.706	0.180	0.840	0.424
		2	0.007	0.108	0.143	0.571
2	0.662	1	0.007	0.108	0.047	0.189
		2	0.543	0.340	0.737	0.583

Proportions of reflected energy for scattering by the fixed end crack in example 3 are reported in Table 4. Note that minor modifications to the theory presented in previous section is required for this problem as the exterior region consists of only one region, which is the reflected field. Reciprocity relation in equation (17b) does not apply for this example problem. At the frequency considered here ($\Omega = 6$), the dispersion relation in equation (4) has three symmetric propagating modes (denoted as 1S, 2S and 3S in Table 4) and four anti-symmetric modes (usually denoted as 1A, 2A, 3A and 4A). It is seen from Table 4 that reciprocity relations among the reflected modes as given in equation (17a) are satisfied with reasonable accuracy for the five different crack lengths considered. In this table, a normalized crack length of 0.0 and 2.0 represent, respectively, the full reflection by a fixed end and reflection by a free end (i.e. a crack right through the full thickness of the plate).

Table 4. Reflected energy proportions E^+_{pn} for example 3 when Ω=6, $\theta = 0^0$, $\varphi^{in} = 0^0$, $\eta_0 = 0$

p, n	E^+_{pn}	a/(0.5H)				
		0.0	0.5	1.0	1.5	2.0
p=1=1S, n=2=2S	E^+_{12}	0.000	0.033	0.001	0.013	0.014
P=2=2S, n=1=1S	E^+_{21}	0.000	0.032	0.001	0.014	0.014
p=1=1S, n=3=3S	E^+_{13}	0.014	0.001	0.038	0.006	0.219
P=3=3S, n=1=1S	E^+_{31}	0.014	0.001	0.040	0.006	0.224
p=1=1S, n=4=1A	E^+_{14}	0.000	0.556	0.567	0.506	0.000
P=4=1A, n=1=1S	E^+_{41}	0.000	0.556	0.557	0.513	0.000

Note: S and A denote symmetric and anti-symmetric modes, respectively.

4. CONCLUSION

Simplified forms of elastodynamic reciprocity relations applicable for guided wave scattering by flaws in fibre-reinforced composite plates have been developed in this work. These relations are useful to check the accuracy of the numerical solution for the scattered wave field in applications involving ultrasonic non-destructive assessment of flaws in composite structures. The classical elastodynamic reciprocity theorem has been used to derive the reciprocity relations for reflected and transmitted wave amplitudes and the corresponding energies associated with the wave modes. A hybrid method combining the finite element method with a wave function expansion procedure has been used to solve the wave scattering problem. The derivation has been presented for a plate with an arbitrary stacking sequence where each ply can have an arbitrary fibre direction. Numerical results verifying the derived reciprocity relations have been presented for three scattering problems – two of them involving scattering by a symmetric normal edge crack in a uni-axially fibre-reinforced composite plate and in an 8-layer cross-ply plate, and other involving a fixed-end crack in a uni-axially fiber-reinforced composite plate.

5. REFERENCES

1. Bakis, C.E., Bank, L.C., Brown, V.L., Cosenza, E., Davalos, J.F., Lesko, J.J., Machida, A. Rizkalla, S.H. and Triantafillou, T.C., "Fiber-reinforced polymer composites for construction – state-of-the-art-Review". *Journal of Composites for Construction; Vol.* 6(2), 2002, pp. 73-87.
2. Chimenti, D. E., "Guided waves in plates and their use in material characterization". *Applied Mechanics Review;* Vol. 50, 1997, pp. 247-284.
3. Datta, S. K., "Wave propagation in composite plates and shells". *Comprehensive Composite Materials;* Vol. 1, 2000, Chapter 18.
4. Karunasena, W., shah, A.H. and Datta, S.K., "Plane strain wave scattering by cracks in laminated composite plates". *Journal of Engineering Mechanics, ASCE;* Vol. 117(8), 1991, 1738-1754.
5. Karunasena, W., "Numerical modelling of obliquely incident guided wave scattering by a crack in a laminated composite plate". *Proceedings of Structural Integrity and Fracture (SIF2004)*, Brisbane, Australia.
6. Karunasena, W, Shah, A H. and Datta, S K, "Reflection of plane strain waves at the free edge of a laminated composite plate". *International Journal of Solids and Structures*; Vol. 27(8), 1991, 949-964.
7. Achenbach, J.D., *Wave Propagation in Elastic Solids.* North Holland, Amsterdam, 1973.
8. Auld, B.A., *Acoustic Fields and Waves in Solids – Vol. 2.* Wiley-Interscience, New York, 1973.
9. Karunasena, W., Bratton, R.L., Shah, A H. and Datta, S. K., "Elastic wave propagation in laminated composite plates". *Journal of Engineering Materials and Technology, ASME*; Vol. 113, 1991, 413-420.